

Inhibition of Neddylolation Modification Sensitizes Pancreatic Cancer Cells to Gemcitabine



Hua Li^{*}, Weihua Zhou^{*}, Lihui Li[§], Jianfu Wu[§], Xiaoli Liu[§], Lili Zhao[¶], Lijun Jia^{#,**} and Yi Sun^{*,†,‡}

^{*}Division of Radiation and Cancer Biology, Department of Radiation Oncology, University of Michigan, 4424B MS-1, 1301 Catherine Street, Ann Arbor, MI 48109, USA; [†]Institute of Translational Medicine, Zhejiang University School of Medicine, Hangzhou, Zhejiang, PR China; [‡]Collaborative Innovation Center for Diagnosis and Treatment of Infectious Diseases, Zhejiang University, Hangzhou, China; [§]Cancer Institute, Fudan University Shanghai Cancer Center, Collaborative Innovation Center of Cancer Medicine, Department of Oncology, Shanghai Medical College, Fudan University, Shanghai, 200032, China; [¶]Department of Biostatistics, University of Michigan, 4424B MS-1, 1301 Catherine Street, Ann Arbor, MI 48109, USA; [#]Oncology Institute of Traditional Chinese Medicine, Shanghai Research Institute of traditional Chinese Medicine, Shanghai 200032, China; ^{**}Department of Oncology, Longhua Hospital Affiliated to Shanghai University of Traditional Chinese Medicine, Shanghai 200032, China

Abstract

Pancreatic ductal adenocarcinoma (PDAC) is the fourth leading cause of cancer death in the USA with a 5-year survival rate less than 3% to 5%. Gemcitabine remains as a standard care for PDAC patients. Although protein neddylation is abnormally activated in many human cancers, whether neddylation dysregulation is involved in PDAC and whether targeting neddylation would sensitize pancreatic cancer cells to gemcitabine remain elusive. Here we report that high expression of neddylation components, NEDD8 and NAE1, are associated with poor survival of PDAC patients. Blockage of neddylation by MLN4924, a small molecule inhibitor targeting this modification, significantly sensitizes pancreatic cancer cells to gemcitabine, as evidenced by reduced growth both in monolayer culture and soft agar, reduced clonogenic survival, decreased invasion capacity, increased apoptosis, G2/M arrest, and senescence. Importantly, combinational treatment of MLN4924-gemcitabine near completely suppressed *in vivo* growth of pancreatic cancer cells. Mechanistically, accumulation of NOXA, a pro-apoptotic protein and ERBIN, a RAS signal inhibitor, appears to play, at least in part, a causal role in MLN4924 chemo-sensitization. Our study demonstrates that neddylation modification is a valid target for PDAC, and provides the proof-of-concept evidence for future clinical trial of MLN4924-gemcitabine combination for the treatment of pancreatic cancer patients.

Neoplasia (2017) 19, 509–518

Introduction

Pancreatic ductal adenocarcinoma (PDAC) is the fourth leading cause of cancer death in the USA and one of the deadliest human malignancies with only 3–5% 5-year survival [1]. Mutational activation of the K-RAS oncogene occurs in 95% of cases, and inactivation of tumor suppressors, p53 and PTEN, occurs at ~50% to 60% of cases [2–4]. In addition, NFκB, a downstream mediator of

Address all correspondence to: Yi Sun, Division of Radiation and Cancer Biology, Department of Radiation Oncology, University of Michigan, 4424B MS-1, 1301 Catherine Street, Ann Arbor, MI 48109, USA.

E-mail: sunyi@umich.edu

Received 14 February 2017; Revised 7 April 2017; Accepted 8 April 2017

© 2017 The Authors. Published by Elsevier Inc. on behalf of Neoplasia Press, Inc. This is an open access article under the CC BY-NC-ND license (<http://creativecommons.org/licenses/by-nc-nd/4.0/>).

1476-5586

<http://dx.doi.org/10.1016/j.neo.2017.04.003>

Table 1. χ^2 Analysis of Patient Clinical Data vs. PDAC IHC Staining

Variable No. (%)	Σ	NAE1		<i>P</i>	NEDD8		<i>P</i>
		low	high		low	high	
Age				1.00			.485
< 60	35 (45.5)	14 (18.2)	21 (27.3)		16 (20.8)	19 (24.7)	
≥ 60	42 (54.5)	16 (20.8)	26 (33.7)		15 (19.5)	27 (35.0)	
Gender				1.00			.642
female	30 (39.0)	12 (15.6)	18 (23.3)		11 (14.3)	19 (24.7)	
male	47 (61.0)	18 (23.4)	29 (37.7)		20 (26.0)	27 (35.0)	
Tumor stage				.087			.342
T1	4 (5.2)	3 (3.9)	1 (1.3)		2 (2.6)	2 (2.6)	
T2	63 (81.8)	21 (27.3)	42 (54.5)		23 (29.9)	40 (51.9)	
T3	10 (13.0)	6 (7.8)	4 (5.2)		6 (7.8)	4 (5.2)	
Node status				1.00			.814
N0	45 (58.4)	18 (23.4)	27 (35.0)		19 (24.7)	26 (33.7)	
N1	32 (41.6)	12 (15.6)	20 (26.0)		12 (15.6)	20 (26.0)	

Table 2. COX Regression Analysis of Patient Clinical Data vs. PDAC IHC Staining

Factors	Univariate Analysis*		Multivariable-Adjusted†	
	HR (95%CI)	<i>P</i>	HR (95%CI)	<i>P</i>
NEDD8				
low expression	1.00 (Reference)		1.00 (Reference)	
high expression	1.82 (1.00–3.29)	.049	2.07 (1.10–3.90)	.023
NAE1				
low expression	1.00 (Reference)		1.00 (Reference)	
high expression	2.38 (1.24–4.57)	.009	1.92 (1.05–3.52)	.035

mutant K-RAS signaling in PDAC [5,6], was constitutively activated in most primary pancreatic cancers and cell lines [7,8], due to at least in part the overexpression of β -TrCP [9], a F-box protein of SCF (SKP1, Cullins, F-box proteins) E3 ligase that recognizes I κ B for targeted degradation [10]. A recent study based upon whole genome sequencing revealed that PDAC has an average of 63 genetic mutations per cancer and involves alterations in 12 distinct signaling pathways [11]. Thus, it is unlikely that drugs that target a single mutated gene product will be effective against PDAC [12].

Protein neddylation is a process of tagging ubiquitin-like molecule NEDD8 (neural precursor cell expressed, developmentally down-

regulated 8) [13], to a lysyl residue of a substrate protein [14,15] through a cascade catalyzed by three enzymes. The E1 NEDD8-activating enzyme (NAE), consisting of NAE1 (also known as APP-BP1) and UBA3 heterodimer; the E2 NEDD8-conjugating enzymes (UBE2M and UBE2F); and the E3 NEDD8 ligases, mainly consisting of a few RING domain-containing proteins, such as RBX1 and RBX2 (for review see [15]). Increasing experimental data have shown that the process of protein neddylation is abnormally activated in a number of human cancers and blockage of this modification by MLN4924, a small molecule inhibitor of NAE [16], has shown anti-cancer efficacy both in preclinical and clinical settings [15,17,18]. However, whether abnormal neddylation modification is involved in PDAC and associated with patient survival remain elusive.

Standard therapy for locally advanced pancreatic cancer is gemcitabine in combination of radiation [19,20]. We have recently shown that MLN4924 significantly sensitized pancreatic cancer cells to radiation both in vitro and in vivo with mechanism involving accumulation of a few SCF substrates, such as CDT1, WEE1, and NOXA, in parallel with an enhancement of radiation-induced DNA damage, aneuploidy, G2/M phase cell-cycle arrest, and apoptosis [21]. Potential additive or synergistic effect of MLN4924 with gemcitabine against pancreatic cancer cells has not been systematically determined.

In this study, we report that two essential components of protein neddylation, namely, NEDD8 and NAE, are highly expressed in PDAC tissues. Importantly, high expression of either protein is significantly associated with poor survival of patients. Using two pancreatic cancer cells lines, we found that MLN4924 significantly sensitizes cancer cells to gemcitabine, as assayed by both in vitro cell culture and in vivo xenograft tumor models, with mechanism involving accumulation of NOXA and ERBIN, further confirmed by siRNA-based rescue experiment. Our study validated that neddylation modification is an attractive therapeutic target for pancreatic cancer and provided a sound rationale for future clinical trial in combination of gemcitabine with MLN4924 for the treatment of this deadly disease.

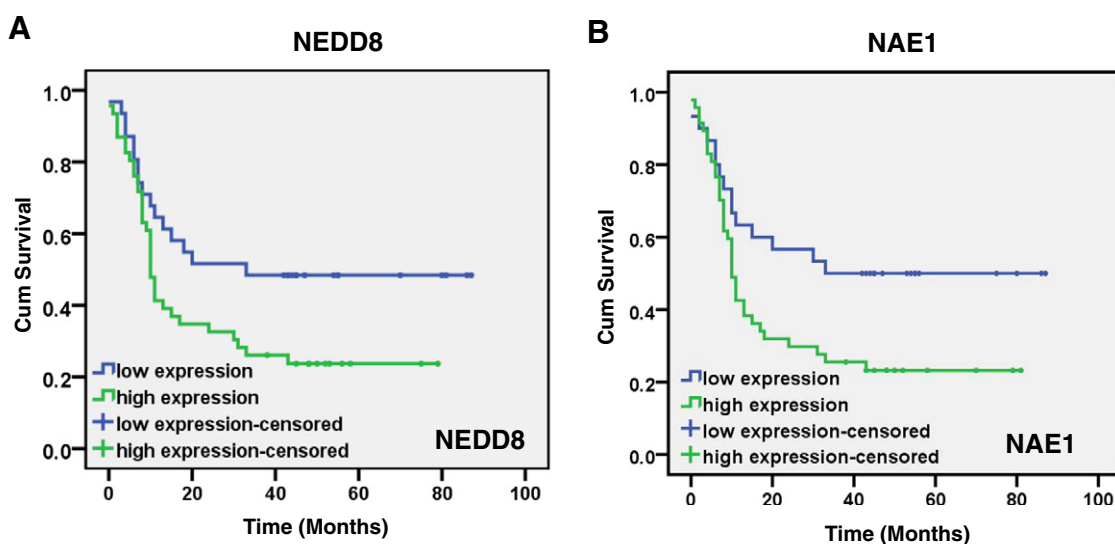


Figure 1. High expression of NEDD8 and NAE1 is associated with poor survival of PDAC patients. Kaplan–Meier curves for overall survival rate of patients with pancreatic cancer according to the expression of NEDD8 (A) and NAE1 (B), respectively (log-rank test). $P < .05$.

Methods

Reagents

The antibodies were purchased from indicated vendors: NEDD8, DEPTOR, pI κ B α , pERK, ERK, pAKT, BIM, pS6K, p4EBP1, and 4EBP1 (Cell Signaling); ERBIN (Novus Biologics); CUL1, I κ B α , AKT, and S6K (Santa Cruz); p21, and p27 (BD Biosciences); NOXA (Millipore), and NAE1 and β -actin (Sigma). The siRNAs targeting NOXA, ERBIN and control siRNA were described previously [22,23]. Immunostaining kit was obtained from DakoCytomation California, Inc. (Carpinteria, CA). ATP-lite kit was obtained from Perkin Elmer (Boston, MA). Boyden chamber for invasion assay was obtained from BD Bioscience (San Jose, CA).

Cell Culture and Growth Assays

Panc-1 and Miapaca-2 cells were purchased from American Type Culture Collection (ATCC). Authentication of 2 cell lines were provided by the Sequencing Core Facility at the University of

Michigan through fragment analysis. DNA profile of two cell lines completely matches with that posted at the ATCC website, respectively.

Cells were cultured in DMEM supplemented with 10% fetal calf serum. Cell growth and survival with or without drug treatment were evaluated by ATP-lite, soft agar and clonogenic assays, as described previously [24–26].

Immunohistochemical (IHC) Staining

Human pancreatic cancer tissue arrays were stained by standard IHC with NAE1 and NEDD8 antibodies by Shanghai Biochip, Shanghai, China. Briefly, the tissue array sections (5 microns) were dehydrated and subjected to peroxidase blocking. Primary antibodies were added and incubated at room temperature for 30 min on the DAKO AutoStainer using the Dako-Cytomation EnVision + System-HRP (DAB) detection kit. The slides were counterstained with hematoxylin. The staining images were acquired under microscopy, and staining intensity was scored from weak (+) to very strong (++++).

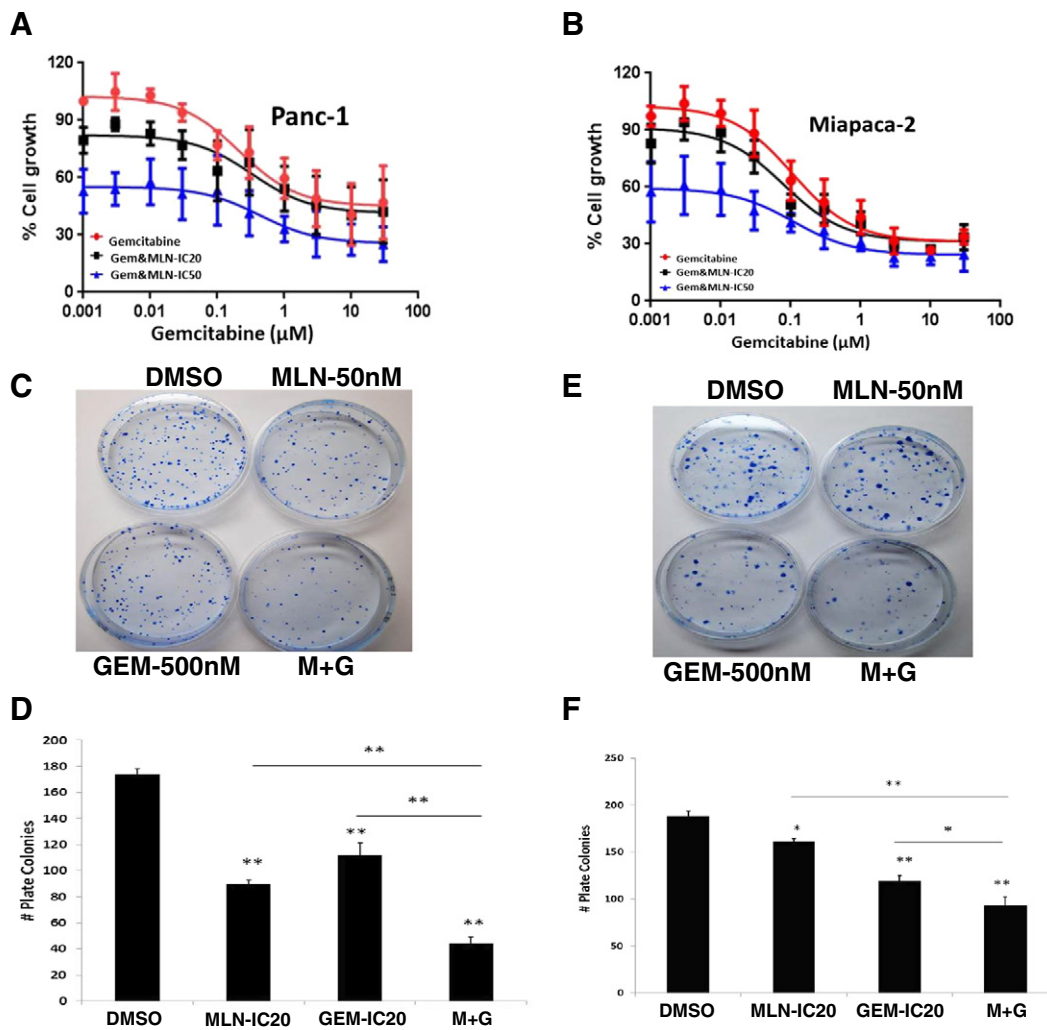


Figure 2. Growth suppression of PDAC cells. (A&B) Inhibition of monolayer growth of PDAC cells: Panc-1 and Miapaca-2 cells were seeded and treated with indicated concentrations of MLN4924 and various concentrations of gemcitabine in 96-well plates (1500 cells/well) in triplicate for 72 h in 10% DMEM. Cells were lysed and subjected to ATP-lite proliferation assay. Shown is $X \pm$ SD of light unit ($n = 2$). (C-F) Inhibition of clonogenic survival: Cells (600) were seeded in 60-mm dish and treated with MLN4924 (for 48 h), gemcitabine (for 4 h) alone or in combination (gemcitabine for 4 h, washed, followed by MLN4924 for 48 h). Cells were then cultured in fresh medium without drugs for additional 10–12 days, and colonies formed were fixed, stained and photographed. The colonies with greater than 50 cells were counted and plotted. Shown is $X \pm$ SEM from three independent experiments, each run in duplicate. Student t test was performed. *, $P < .05$; **, $P < .01$.

Tissue Collection, Clinicopathological Characteristics of Patients, and Data Analysis

All patients underwent surgery treatments in accordance with clinical practice guidelines by the National Comprehensive Cancer Network (NCCN). Fresh primary pancreatic cancer tissues and adjacent pancreatic tissues were collected from 77 pancreatic carcinoma patients undergoing resection from December 2004 to December 2007, at the Taizhou Hospital (Taizhou, China). Histological diagnosis and tumor-node-metastasis (TNM) stages of cancer were determined in accordance with the criteria by the American Joint Committee on Cancer (AJCC) manual for pancreatic cancer. Written informed consent regarding tissue and data usage for scientific purposes was obtained from all participating patients. The study was approved by the Research Ethics Committee of Taizhou Hospital. Patient information and tissue sources were provided by Shanghai Biochip from which tissue microarrays were purchased.

Data are presented as mean \pm SD and the Student *t* test was used for the comparison of parameters between two groups. Survival was analyzed using the Kaplan–Meier method and compared by the log-rank test. The Cox proportional hazards model was used to calculate hazard ratios (HRs) and their corresponding 95% confidence intervals (CIs) with adjustment for potential confounders. SAS software, version 9.2 (SAS Institute, Inc., Cary, NC, USA) and Statistical Program for Social Sciences (SPSS) software 17.0 (SPSS Inc., Chicago, IL, USA) were used for statistical analyses. All statistical tests were two-sided.

Fluorescence Activated Cell Sorting (FACS)

FACS analysis was performed as described [27]. Briefly, cells after treatment with MLN4924 or gemcitabine, alone or combination for various time periods were harvested and fixed in 70% ethanol at -20°C for at least 4 h. Cells were then suspended in 1 x Propidium Iodide solution with 400 mg/ml RNase (Roche), and analyzed in the Flow Cytometry Lab facility at the University of Michigan. The percent of apoptosis is the percentage of cells in the sub-G1 population. The percentage of cells at each phase of cell cycle was recorded and plotted.

SA- β -Galactosidase Staining for Senescence

The pancreatic cancer cells were seeded in 6-well plate, and treated with MLN4924 or gemcitabine alone or in combination for 48 h. Cells were then subjected to SA- β -gal staining, as described [28].

Invasion Assay

The Boyden chamber invasion assay (BD Biosciences) was performed according to manufacturer's instruction. Briefly, cells were seeded in the upper chamber with serum-free DMEM containing MLN4924 or gemcitabine, alone or in combination. The bottom chamber contained 10% DMEM without drugs. Cells were incubated at 37°C for 48 h, then fixed in 100% methanol for 2 min, stained with 1% toluidine and 1% borax solution for 2 min. Cells in five fields on each filter were photographed at $40\times$ magnification and counted. Percentage of invasion was calculated as

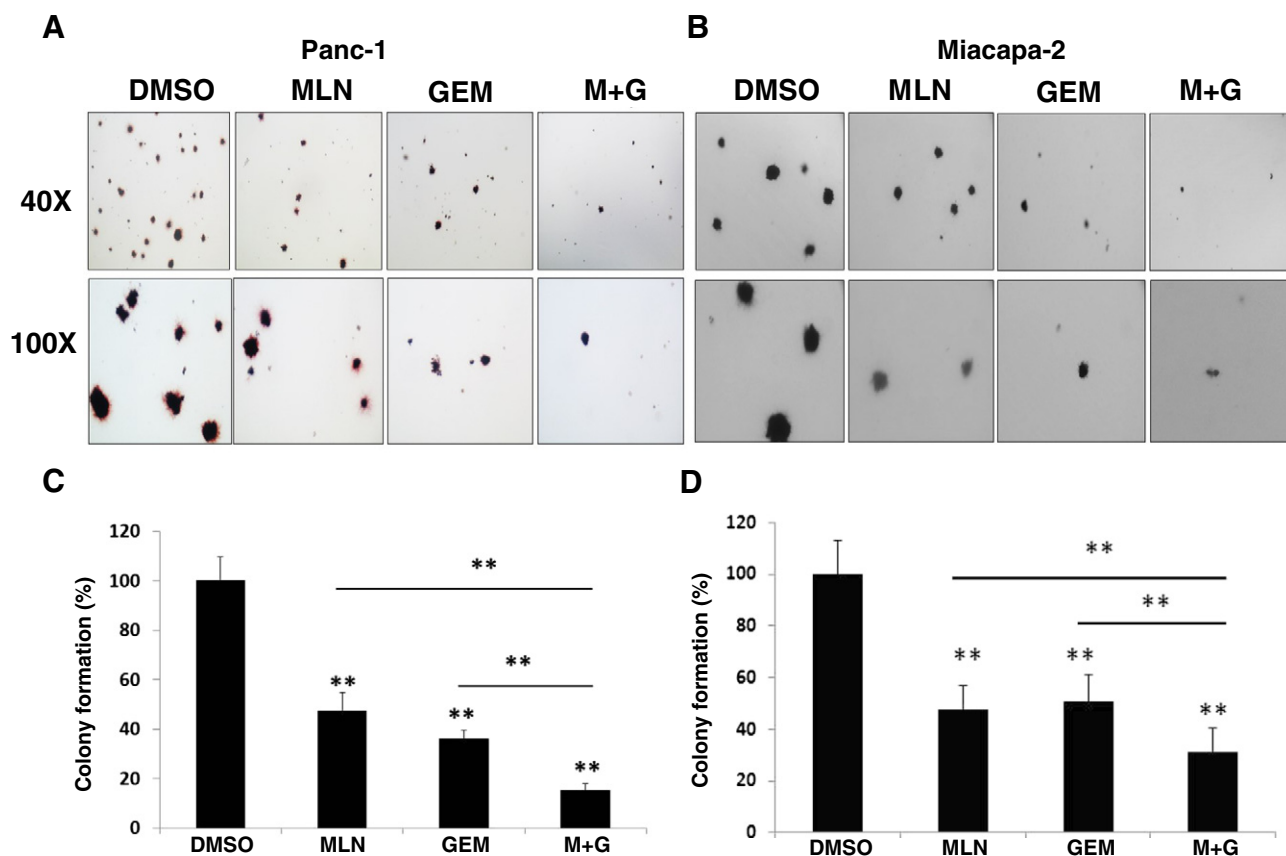


Figure 3. Inhibition of anchorage-independent growth of PDAC cells: Single cell suspension of Panc-1 and Miapaca-2 cells were seeded into 60-mm agar dishes (1.5×10^4 cells/dish) containing the drug concentrations at the IC_{20} (50 nM MLN4924, 80 nM Gemcitabine for Panc-1 cells; 20 nM MLN4924, 80 nM Gemcitabine for Miapaca-2), alone or in combination. Colonies (≥ 8 cells) were counted after 14 days and photographed (A&B). Quantified results were expressed as percentage to the DMSO control, setting at 100% (C&D). Shown is $X \pm \text{SEM}$ ($n = 3$). Student *t* test was performed, **, $P < .01$.

follows: Invasion (%) = (mean# of cells invading through Matrigel insert in drug treated groups) ÷ (mean# of cells migrating through DMSO-treated insert) × 100.

siRNA-Based Knockdown

PANC1 and Miapaca-2 cells were transfected by Lipofectamine 2000 with siRNA oligonucleotide, specifically targeting ERBIN [23] or NOXA, along with scrambled control (siCon) [22]. Cells were harvested 48 h post-transfection and subjected to western blotting or clonogenic assay.

Western Blotting Analysis

Sub-confluent cells after treatment with MLN4924 or gemcitabine, alone or in combination for various time periods were harvested and subjected to Western blotting analysis.

In Vivo Anti-Tumor Growth

All animal studies were conducted in accordance with the guidelines established by the University Committee on Use and Care of Animals. Five million MiaPaCa-2 cells were inoculated subcutaneously into nude mice (6 per group, except for control group, which has 14). The mice were randomized and the treatment started when the tumor size reached 100 mm³ at 14 days after inoculation. MLN4924 (30 mg/kg, s.c.) were given once a day, 5 days

a week, whereas gemcitabine (120 mg/kg, s.c.) was given once a week, alone or in combination for 7 weeks. The growth of tumors was measured twice a week for 7 weeks, and average tumor volumes were calculated, as estimated from the formula $(L \times W^2)/2$. At the end of experiment, tumors were harvested, weighed, and photographed.

Linear mixed effects model was used to compare tumor growth rates between treatment groups based on log-transformed tumor volumes measured over time. The model includes a random intercept and a random slope to allow each tumor has its own growth profile. The fit of the model was visually checked by various residual plots. Additionally, we compared tumor volume doubling times between treatment groups. Tumor volume doubling was determined for each xenograft by identifying the earliest day on which it was at least twice as large as on the first day of treatment. A cubic smoothing spline was used to obtain the exact time of doubling. Then the doubling times were estimated using Kaplan–Meier methods and compared between groups using Log-rank tests. ANOVA (one-way analysis of variance) was used to compare animals' weights followed by the Tukey's test for the multiple comparisons. All analyses were conducted using SAS (version 9.4, SAS Institute, Cary, NC). $P < .05$ was considered statistically significant.

B-Spline basis functions were used to estimate the cell growth curves (Figure 2, A and B) and the spline basis generated for each

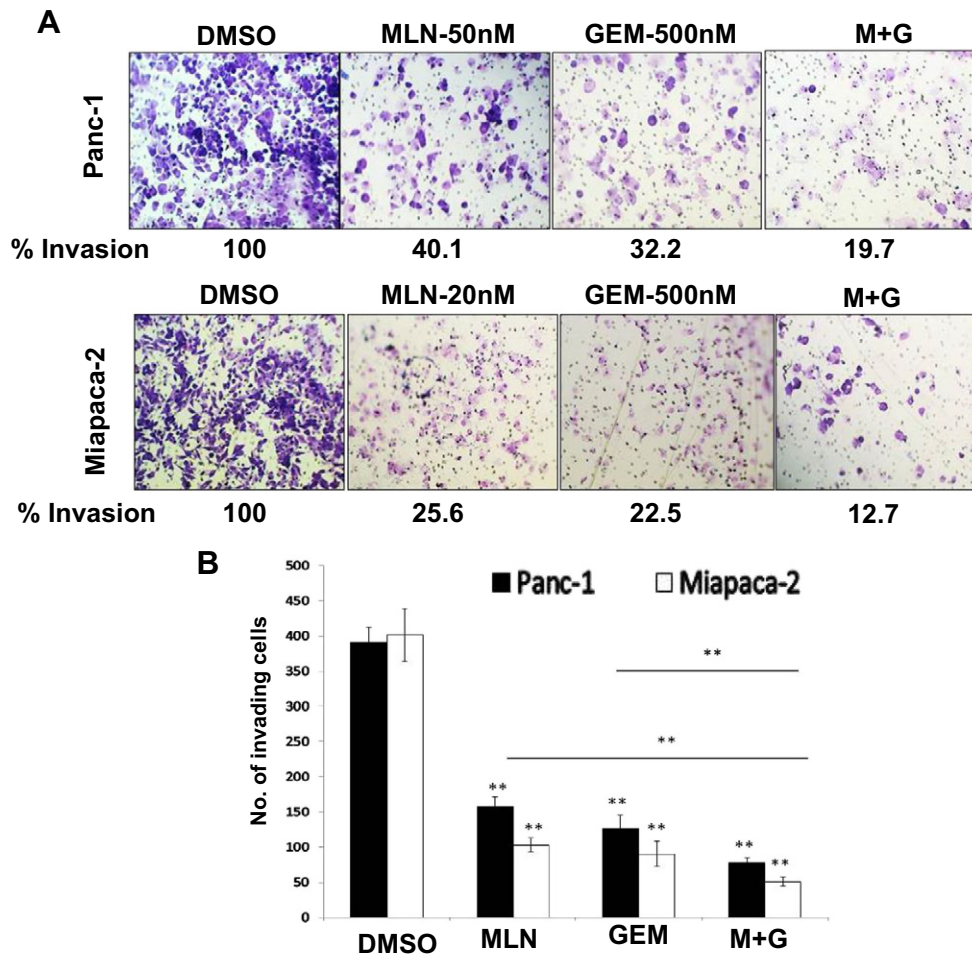


Figure 4. Inhibition of invasion. Panc-1 and Miapaca-2 cells (6×10^4) were seeded into upper chamber of Boyden chamber with serum-free media containing indicated concentrations of MLN4924 (for 48 h) or gemcitabine (4 h), alone or in combination (Gemcitabine for 4 h, washed, then MLN4924 for 48 h). The bottom chamber contained 10% DMEM without drugs. In the end of experiments, cells were fixed, stained and counted using DMSO control setting at 100%. Shown are $X \pm SD$ ($n = 2$). Student t test was performed, **, $P < .01$.

variable is a cubic B-spline basis with three equally spaced knots positioned between the minimum and maximum values of that variable [29]. PROC GLIMMIX in SAS was used to estimate the curves and make comparisons between treatment groups. In the regression model, there is a main effect of treatment group, which creates separate intercepts for the groups, and an interaction of the group variable with the spline effect creates separate trends. The comparisons at each dose were derived from the regression model.

Results and Discussion

High Levels of NEDD8 and NAE1 in PDAC Tissues are Correlated with Poor Patient Survival

Our previous studies have shown a positive correlation between overexpression of NEDD8 and NAE1, two essential neddylation components, and poor prognosis in patients with cancers in the lung [30], liver [31], intrahepatic cholangiole [32], esophagus [33], and brain [34]. Here we extended these studies to human pancreatic ductal adenocarcinoma (PDAC) by using immunohistochemical staining (IHC) to measure the protein levels of NEDD8 and NAE1 in PDAC tissues ($n = 77$). We scored the intensity of IHC staining from the low (+) to medium (++), strong (+++) and very strong (++++). (Figure S1).

We then performed X^2 analysis of staining intensity of these two proteins vs. patient clinical characteristic and found no correlation with patient age, sex, tumor stages and node status (Table 1). The univariable COX regression analysis, however, revealed that high expression of NEDD8 or NAE1 is associated with poor overall

survival of PDAC patients (Table 2). Importantly, multivariable cox regression analysis identified both NEDD8 and NAE1 as independent prognostic factor for overall survival of pancreatic carcinoma patients (Table 2). Moreover, Kaplan–Meier analysis showed that the overall survival rate was statistically significantly lower in PDAC patients with high expression of NEDD8 (Figure 1A, $P < .041$, $n = 77$) or NAE1 (Figure 1B, $P < .028$, $n = 77$) than that in patients with low expression of these proteins, respectively. Thus, it appears that high expression of NEDD8 and NAE1 in pancreatic cancer is significantly associated with worse prognosis of patients.

MLN4924 Sensitizes Pancreatic Cancer Cells to Gemcitabine

We next determined whether inactivation of neddylation modification by MLN4924, a small molecule inhibitor of NAE [16], would enhance growth suppression by gemcitabine. We first used a standard cell growth ATP-lite assay to generate IC_{50} curve of MLN4924 and gemcitabine against both Panc-1 and Miapaca-2 pancreatic cancer cells (Figure S2, A and B). The IC_{20} and IC_{50} concentrations of MLN4924, along with the vehicle control, were used in combination of various concentrations of gemcitabine to generate a growth suppression curve. Indeed, a dose dependent growth suppression was observed by gemcitabine alone treatment. Addition of MLN4924 either at concentrations of IC_{20} or IC_{50} caused the greater growth inhibition, which is also in a dose dependent manner (Figure 2, A and B). The difference was statistically significant at low gemcitabine concentrations (Table S1). However, the combination appears to cause an additive effect with a maximal

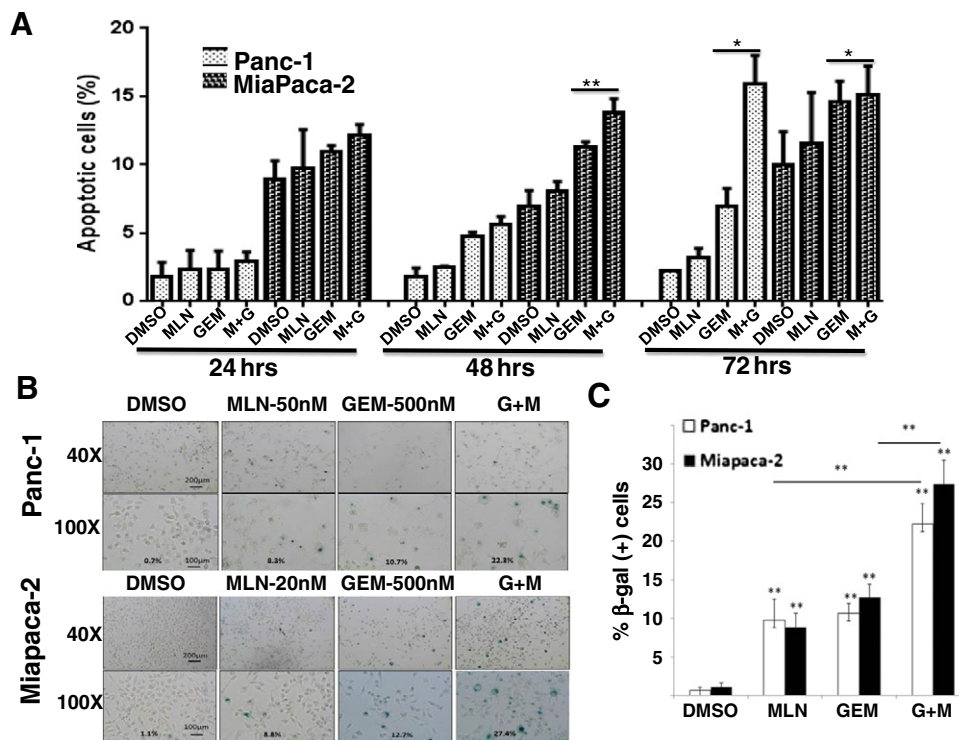


Figure 5. Induction of apoptosis and senescence: Panc-1 and Miapaca-2 cells were seeded into 60-mm dishes and treated with MLN4924 (50 nM for Panc-1, 20 nM for Miapaca-2) for up to 72 h; or Gemcitabine (500 nM) for first 4 h or the combination (Gemcitabine 4 h, MLN4924 for up to 72 h) at 10% DMEM. Every 24 h post drug treatment, cells were harvested and prepared for FACS analysis. Sub-G1 population was used to calculate % of apoptotic cells (A). Cells were seeded in cover slide, followed by drug treatment as indicated above for 48 h. Cells were stained with β -Gal for 24–48 h and blue cells were counted. Quantified results were expressed as percentage of β -Gal (+) cells to the DMSO control, setting at 100% (B&C). Shown is $X \pm SD$ ($n = 2$). Student t test was performed. *, $P < .05$; **, $P < .01$.

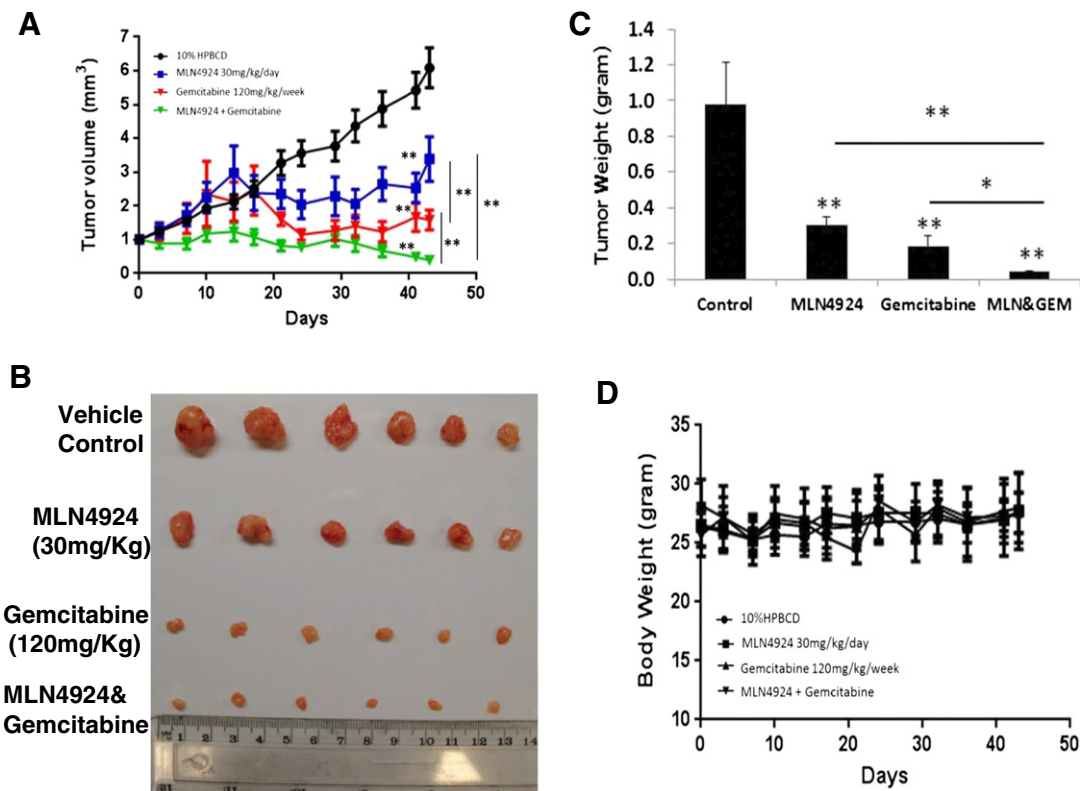


Figure 6. Inhibition of *in vivo* tumor growth. Five million of MiaPaCa-2 cells were inoculated subcutaneously in both flanks of nude mice. The mice were randomized and the treatment started when the tumor size reached 100 mm³ at 14 days after inoculation. Animals were dosed as indicated for 5 weeks. The growth of tumors (6 for each group) was measured twice a week for 7 weeks, and results plotted (A). Tumors were harvested and photographed (B) and weighed with results plotted (C). The weight of animals was monitored twice a week and results plotted (D). Shown is X ± SEM. Statistical analysis was detailed in the M&M. *, *P* < .05; **, *P* < .01.

suppression reaching up to 70–80% (Figure 2, A and B). We also performed clonogenic assay to determine the effect of MLN4924 on survival of pancreatic cells, alone or in combination with gemcitabine. And again, the combination caused the highest suppression (Figure 2, C–F). We further used soft agar assay to determine the effect of MLN4924 on anchorage independent growth, alone or in combination with gemcitabine. Indeed, the combination caused significantly more growth suppression in both cancer cell lines (Figure 3, A–D). Thus, MLN4924 sensitized pancreatic cancer cells to gemcitabine.

Enhanced Suppression of Invasion by Combination of MLN4924 and Gemcitabine

We next determined the effect of MLN4924, alone or in combination with gemcitabine, on invasion capacity of pancreatic cancer cells. In Panc-1 cells, MLN4924 at 50 nM caused 60% inhibition, whereas gemcitabine at 500 nM caused ~70% inhibition. The combination of both induced 80% inhibition which was statistically significant (Figure 4, A and B). Likewise, in MiaPaca-2 cells, single drug treatment caused ~75% inhibition, whereas the combination caused up to 90% inhibitions, which is again statistically significant (Figure 4, A and B). Thus, MLN4924 alone suppressed invasion of pancreatic cancer cells as well as enhanced the effect of gemcitabine.

MLN4924 Gemcitabine Sensitization is Mediated by Induction of Apoptosis, G2/M Arrest, and Senescence

We then determined the nature of growth suppression using FACS analysis. Cells were grown in monolayer culture for up to 3 days with

samples harvested at every 24 h. Apoptotic cells were indexed by sub-G1 population. FACS profile revealed that MLN4924 failed to induce apoptosis, whereas gemcitabine caused minor induction. Combination of both drugs caused significantly more induction of apoptosis in a time dependent manner: the longer treatment period and the greater apoptosis induction (Figure 5A). Compared to gemcitabine alone treatment, the combinational treatment caused significant induction G2/M arrest in both pancreatic cell lines (Figure S3). Furthermore, using β-gal staining as the readout, we observed induction of senescence in both lines by each individual treatment, and the combinational treatment caused the maximal induction of senescence (Figure 5, B and C). Thus, the growth suppression induced by two drugs alone or in combination appears to be mediated by the induction of apoptosis, G2/M arrest and senescence.

Enhanced Suppression of In Vivo Tumor Growth by MLN4924-Gemcitabine Combination

Finally, we used xenograft tumor model of MiaPac-2 cells and determined the effect of two drugs alone or in combination on *in vivo* tumor growth in nude mice [21]. Tumor growth was moderately inhibited by the treatment with MLN4924 (30 mg/kg, 5 times per week), more significantly inhibited by the treatment with gemcitabine (120 mg/kg, once a week). A near complete growth inhibition was achieved in combinational treatment (Figure 6A, Figure S4). Analysis of weight of tumor mass harvested at the end of experiment showed a statistical difference between alone and combinational

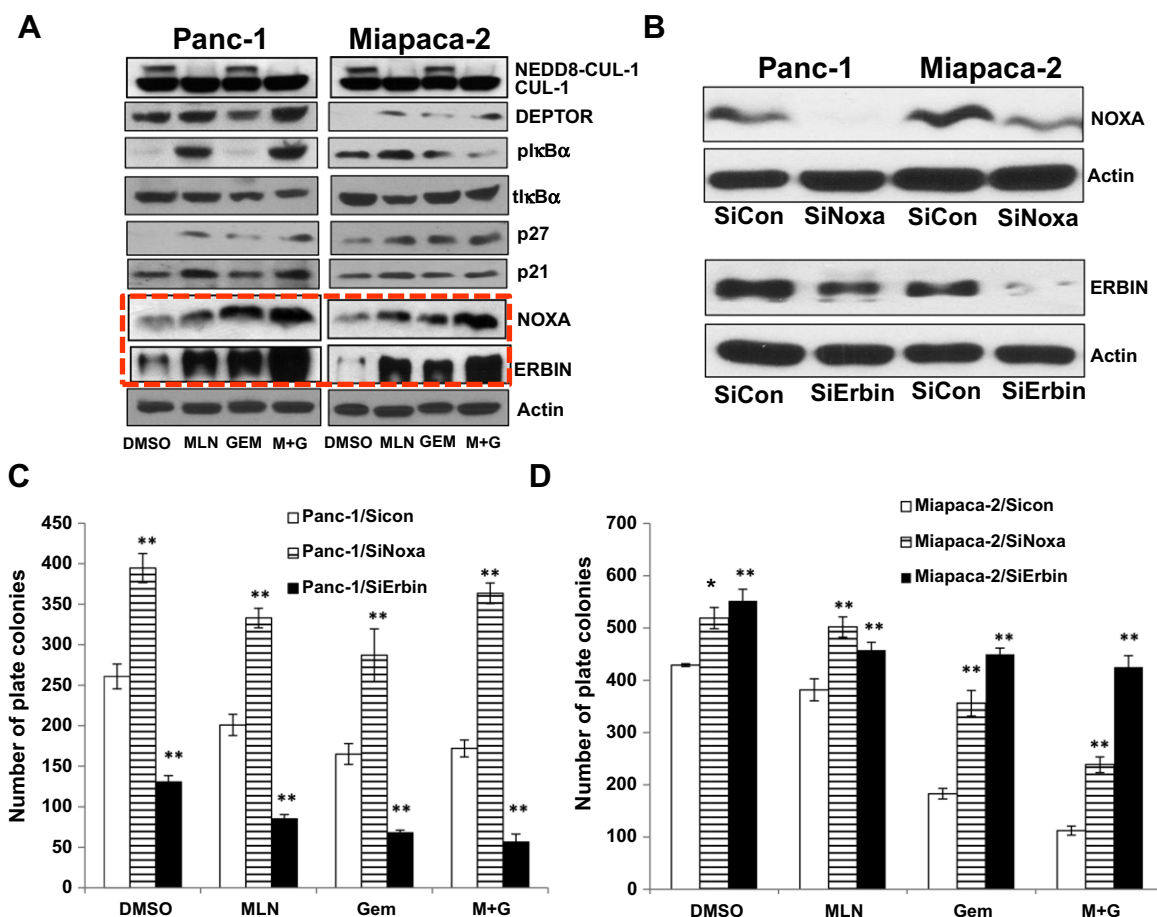


Figure 7. MLN4924-induced accumulation of NOXA and ERBIN plays a causal role in gemcitabine sensitization. Panc-1 and Miapaca-2 cells were seeded into 60-mm dishes and treated with MLN4924, gemcitabine alone or in combination as described in Figure 5 legend. Cells were harvested after being cultured at 10% DMEM for 48 h before being lysed for Western blotting analysis using indicated antibodies (A). PANC-1 and Miapaca-2 cells were seeded into 6-well plates and transfected with siRNA targeting NOXA (siNOXA) or Erbin (siErbin), along with scrambled control (siCon) for 6 h. After transfection, cells were split for drug treatment as described in Figure 2 legend for 48 h, and harvested for Western blotting (B), or cultured for additional 10–12 days for clonogenic growth (C&D). Colonies were stained and counted. Shown is $X \pm \text{SEM}$ ($n = 3$). Student *t* test was performed. *, $P < .05$; **, $P < .01$, as compared to siCon group. Note that much longer exposure was conducted in (B) than (A) for ERBIN detection.

group (Figure 6, B and C). Finally, the dosage used was not toxic to the animals as judged by a minimal loss of body weight (Figure 6D). Taken together, the results demonstrated that MLN4924 indeed sensitizes pancreatic cancer cells to gemcitabine, using both in vitro cell culture and in vivo xenograft tumor model.

Mechanism of MLN4924 Action

Activity of Cullin RING ligase (CRL) requires cullin neddylation, which is inhibited by MLN4924 [16]. To elucidate potential mechanistic action of MLN4924 as a gemcitabine sensitizer, we first focused on few growth-regulatory substrates of CRL1 (also known as SCF) E3 ligase with expected accumulation. We first confirmed that MLN4924 indeed inhibited cullin neddylation (Figure 7A top panel) and caused accumulations in both cell lines of DEPTOR, an mTOR inhibitor; pIκBα, an inhibitor of NFκB; p21 and p27, two inhibitors of cyclin dependent kinases [15,18] (Figure 7A). However, we did not see further accumulations of these proteins in combinational treatment (Figure 7A), suggesting that it is unlikely that these proteins will play a critical role in chemo-sensitization. On the other hand, we did observe combinational treatment caused higher accumulation of (a) NOXA, a pro-apoptotic protein, shown to be a CRL5 substrate [22,35], and (b) ERBIN, a natural

occurring inhibitor of RAS-MAPK pathway [36,37], a recently characterized substrate of SAG-CRL1 [23] in both pancreatic cancer cell lines (Figure 7A). Given the fact that NOXA is a p53 transcriptional target [38], whereas both Panc-1 and Miapaca-2 cells harbors mutant p53 [39,40], the drug-induced NOXA accumulation is likely p53-independent, rather due to inhibition of cullin-RING ligase activity to block its degradation in case of MLN4924 effect.

We next performed rescue experiment to elucidate if accumulated NOXA or ERBIN is causally related to MLN4924 gemcitabine sensitization via siRNA-based knockdown (Figure 7B), followed by clonogenic survival assay (Figure 7, C and D, Figure S5, A and B). In Panc-1 cells, while ERBIN knockdown significantly inhibited colony survival alone or in combination of MLN4924 or gemcitabine, NOXA knockdown stimulated it and rescued suppressive effect of either drug alone, or in combination (Figure 7C, Figure S5A). In Miapaca-2 cells, knockdown of either NOXA or ERBIN stimulated colony survival and rescued drug inhibitory effect alone or in combination (Figure 7D, Figure S5B). Taken together, our results suggest that MLN4924-induced accumulation of NOXA plays a causal role in gemcitabine sensitization, whereas ERBIN acts in a cell-line dependent manner to overcome gemcitabine resistance by blocking MAPK signals [41].

MLN4924 belongs to the same drug category as Velcade (also known as Bortezomib or PS-341), the first class of general proteasome inhibitor, approved by the FDA for the treatment of relapsed/refractory multiple myeloma and mantle cell lymphoma [42]. Given Velcade is a general inhibitor of proteasomes that inhibits the degradation of a wide array of cellular proteins, the drug toxicity is high which has limited its utility due to many associated side-effects [43]. In contrast, by inhibiting cullin neddylation, MLN4924 selectively inhibits only cullin-RING E3 ubiquitin ligases (CRLs) [16], with anticipated lesser toxicity. Due to its high potency against many types of human cancers, and less toxicity in normal cells in preclinical setting, MLN4924 is currently being advanced to several Phase I/II clinical anticancer trials [15] (<http://www.cancer.gov/search/ResultsClinicalTrials.aspx?protocolsearchid=7656926>). Our previous study showed that MLN4924 sensitized pancreatic cancer cells to radiation [21]. Here we showed that MLN4924 can act as a potent chemo-sensitizer as well to enhance the effect of gemcitabine against pancreatic cancer cells by inducing apoptosis, which is causally related to NOXA accumulation. Our study provides proof-of-concept evidence for future clinical trial of gemcitabine-MLN4924 combination to treat pancreatic cancer.

Authors' Contributions

H.L., L.J. and Y.S. conceived and designed the experiments. H.L., W.Z., L.L., and J.W. performed the experiments. H.L., X.L., L.Z. and Y.S. analyzed the data. Y.S. wrote the paper. All authors critically discussed the results, and reviewed and approved the manuscript before submission.

Acknowledgements

We would like to thank Takeda Pharmaceuticals, Inc. for providing us MLN4924 as well as financial support. This work was also supported by the NCI grants (CA156744, and CA171277) and by the Chinese NSFC Grants 81572718, and by the Chinese Minister of Science and Technology grant 2016YFA0501800 to YS. The author (YS) also gratefully acknowledges the support of K. C. Wong Education Fund.

Appendix A. Supplementary data

Supplementary data to this article can be found online at <http://dx.doi.org/10.1016/j.neo.2017.04.003>.

References

- Jemal A, Siegel R, Xu J, and Ward E (2010). Cancer Statistics, 2010. *CA Cancer J Clin*.
- Hezel AF, Kimmelman AC, Stanger BZ, Bardeesy N, and Depinho RA (2006). Genetics and biology of pancreatic ductal adenocarcinoma. *Genes Dev* **20**, 1218–1249.
- Morris JPt, Wang SC, and Hebrok M (2010). KRAS, Hedgehog, Wnt and the twisted developmental biology of pancreatic ductal adenocarcinoma. *Nat Rev Cancer* **10**, 683–695.
- Asano T, Yao Y, Zhu J, Li D, Abbruzzese JL, and Reddy SA (2004). The PI 3-kinase/Akt signaling pathway is activated due to aberrant Pten expression and targets transcription factors NF-kappaB and c-Myc in pancreatic cancer cells. *Oncogene* **23**, 8571–8580.
- Sclabas GM, Fujioka S, Schmidt C, Evans DB, and Chiao PJ (2003). NF-kappaB in pancreatic cancer. *Int J Gastrointest Cancer* **33**, 15–26.
- Zhang Z and Rigas B (2006). NF-kappaB, inflammation and pancreatic carcinogenesis: NF-kappaB as a chemoprevention target (review). *Int J Oncol* **29**, 185–192.
- Wang W, Abbruzzese JL, Evans DB, Larry L, Cleary KR, and Chiao PJ (1999). The nuclear factor-kappa B RelA transcription factor is constitutively activated in human pancreatic adenocarcinoma cells. *Clin Cancer Res* **5**, 119–127.
- Chandler NM, Canete JJ, and Callery MP (2004). Increased expression of NF-kappa B subunits in human pancreatic cancer cells. *J Surg Res* **118**, 9–14.
- Muerkoster S, Arlt A, Sipos B, Witt M, Grossmann M, Kloppel G, Kalthoff H, Folsch UR, and Schafer H (2005). Increased expression of the E3-ubiquitin ligase receptor subunit betaTRCP1 relates to constitutive nuclear factor-kappaB activation and chemoresistance in pancreatic carcinoma cells. *Cancer Res* **65**, 1316–1324.
- Tan M, Zhu Y, Kovacev J, Zhao Y, Pan ZQ, Spitz DR, and Sun Y (2010). Disruption of Sag/Rbx2/Roc2 induces radiosensitization by increasing ROS levels and blocking NF-kB activation in mouse embryonic stem cells. *Free Radic Biol Med* **49**, 976–983.
- Jones S, Zhang X, Parsons DW, Lin JC, Leary RJ, Angenendt P, Mankoo P, Carter H, Kamiyama H, and Jimeno A, et al (2008). Core signaling pathways in human pancreatic cancers revealed by global genomic analyses. *Science* **321**, 1801–1806.
- Koorstra JB, Hustinx SR, Offerhaus GJ, and Maitra A (2008). Pancreatic carcinogenesis. *Pancreatology* **8**, 110–125.
- Kamitani T, Kito K, Nguyen HP, and Yeh ET (1997). Characterization of NEDD8, a developmentally down-regulated ubiquitin-like protein. *J Biol Chem* **272**, 28557–28562.
- Watson IR, Irwin MS, and Ohh M (2011). NEDD8 pathways in cancer, Sine Quibus Non. *Cancer Cell* **19**, 168–176.
- Zhao Y, Morgan MA, and Sun Y (2014). Targeting Neddylation Pathways to Inactivate Cullin-RING Ligases for Anticancer Therapy. *Antioxid Redox Signal* **21**, 2383–2400.
- Soucy TA, Smith PG, Milhollen MA, Berger AJ, Gavin JM, Adhikari S, Brownell JE, Burke KE, Cardin DP, and Critchley S, et al (2009). An inhibitor of NEDD8-activating enzyme as a new approach to treat cancer. *Nature* **458**, 732–736.
- Nawrocki ST, Griffin P, Kelly KR, and Carew JS (2012). MLN4924: a novel first-in-class inhibitor of NEDD8-activating enzyme for cancer therapy. *Expert Opin Investig Drugs* **21**, 1563–1573.
- Zhao Y and Sun Y (2013). Cullin-RING Ligases as Attractive Anti-cancer Targets. *Curr Pharm Des* **19**, 3215–3225.
- Hidalgo M (2010). Pancreatic cancer. *N Engl J Med* **362**, 1605–1617.
- Morgan MA, Parsels LA, Maybaum J, and Lawrence TS (2008). Improving gemcitabine-mediated radiosensitization using molecularly targeted therapy: a review. *Clin Cancer Res* **14**, 6744–6750.
- Wei D, Li H, Yu J, Sebolt JT, Zhao L, Lawrence TS, Smith PG, Morgan MA, and Sun Y (2012). Radiosensitization of human pancreatic cancer cells by MLN4924, an investigational NEDD8-activating enzyme inhibitor. *Cancer Res* **72**, 282–293.
- Zhou W, Xu J, Li H, Xu M, Chen ZJ, Wei W, Pan ZQ, and Sun Y (2017). Neddylation E2 UBE2F promotes the survival of lung cancer cells by activating CRL5 to degrade NOXA via the K11 linkage. *Clin Cancer Res* **23**, 1104–1116.
- Xie CM, Wei D, Zhao L, Marchetto S, Mei L, Borg JP, and Sun Y (2015). Erbin is a novel substrate of the Sag-betaTrCP E3 ligase that regulates KrasG12D-induced skin tumorigenesis. *J Cell Biol* **209**, 721–738.
- Gu Q, Tan M, and Sun Y (2007). SAG/ROC2/Rbx2 is a novel activator protein-1 target that promotes c-Jun degradation and inhibits 12-O-tetradecanoylphorbol-13-acetate-induced neoplastic transformation. *Cancer Res* **67**, 3616–3625.
- Sun SH, Zheng M, Ding K, Wang S, and Sun Y (2008). A small molecule that disrupts Mdm2-p53 binding activates p53, induces apoptosis, and sensitizes lung cancer cells to chemotherapy. *Cancer Biol Ther* **7**, 845–852.
- Li H, Sun GY, Zhao Y, Thomas D, Greenson JK, Zalupski MM, Ben-Josef E, and Sun Y (2014). DEPTOR has growth suppression activity against pancreatic cancer cells. *Oncotarget* **5**, 12811–12819.
- Bockbrader KM, Tan M, and Sun Y (2005). A small molecule Smac-mimic compound induces apoptosis and sensitizes TRAIL- and etoposide-induced apoptosis in breast cancer cells. *Oncogene* **24**, 7381–7388.
- Jia L, Li H, and Sun Y (2011). Induction of p21-Dependent Senescence by an NAE Inhibitor, MLN4924, as a Mechanism of Growth Suppression. *Neoplasia* **13**, 561–569.
- Eilers PHC and Marx BD (1996). Flexible smoothing with B-splines and penalties. *Stat Sci* **11**, 89–121.
- Li L, Wang M, Yu G, Chen P, Li H, Wei D, Zhu J, Xie L, Jia H, and Shi J, et al (2014). Overactivated neddylation pathway as a therapeutic target in lung cancer. *J Natl Cancer Inst* **106**, dju083.
- Luo Z, Yu G, Lee HW, Li L, Wang L, Yang D, Pan Y, Ding C, Qian J, and Wu L, et al (2012). The Nedd8-Activating Enzyme Inhibitor MLN4924 Induces Autophagy and Apoptosis to Suppress Liver Cancer Cell Growth. *Cancer Res* **72**, 3360–3371.
- Gao Q, Yu GY, Shi JY, Li LH, Zhang WJ, Wang ZC, Yang LX, Duan M, Zhao H, and Wang XY, et al (2014). Neddylation pathway is up-regulated in human intrahepatic cholangiocarcinoma and serves as a potential therapeutic target. *Oncotarget* **5**, 7820–7832.

- [33] Chen P, Hu T, Liang Y, Li P, Chen X, Zhang J, Ma Y, Hao Q, Wang J, and Zhang P, et al (2016). Neddylation Inhibition Activates the Extrinsic Apoptosis Pathway through ATF4-CHOP-DR5 Axis in Human Esophageal Cancer Cells. *Clin Cancer Res* **22**, 4145–4157.
- [34] Hua W, Li C, Yang Z, Li L, Jiang Y, Yu G, Zhu W, Liu Z, Duan S, and Chu Y, et al (2015). Suppression of glioblastoma by targeting the overactivated protein neddylation pathway. *Neuro Oncol* **17**, 1333–1343.
- [35] Jia L, Yang J, Hao X, Zheng M, He H, Xiong X, Xu L, and Sun Y (2010). Validation of SAG/RBX2/ROC2 E3 Ubiquitin Ligase as an Anticancer and Radiosensitizing Target. *Clin Cancer Res* **16**, 814–824.
- [36] Dai P, Xiong WC, and Mei L (2006). Erbin inhibits RAF activation by disrupting the sur-8-Ras-Raf complex. *J Biol Chem* **281**, 927–933.
- [37] Kolch W (2003). Erbin: sorting out ErbB2 receptors or giving Ras a break? *Sci STKE* **2003**, pe37.
- [38] Oda E, Ohki R, Murasawa H, Nemoto J, Shibue T, Yamashita T, Tokino T, Taniguchi T, and Tanaka N (2000). Noxa, a BH3-only member of the Bcl-2 family and candidate mediator of p53-induced apoptosis. *Science* **288**, 1053–1058.
- [39] Lang D, Miknyoczki SJ, Huang L, and Ruggeri BA (1998). Stable reintroduction of wild-type P53 (MTmp53ts) causes the induction of apoptosis and neuroendocrine-like differentiation in human ductal pancreatic carcinoma cells. *Oncogene* **16**, 1593–1602.
- [40] Kobayashi D, Sasaki M, and Watanabe N (2001). Caspase-3 activation downstream from reactive oxygen species in heat-induced apoptosis of pancreatic carcinoma cells carrying a mutant p53 gene. *Pancreas* **22**, 255–260.
- [41] Miyabayashi K, Ijichi H, Mohri D, Tada M, Yamamoto K, Asaoka Y, Ikenoue T, Tateishi K, Nakai Y, and Isayama H, et al (2013). Erlotinib prolongs survival in pancreatic cancer by blocking gemcitabine-induced MAPK signals. *Cancer Res* **73**, 2221–2234.
- [42] Kane RC, Bross PF, Farrell AT, and Pazdur R (2003). Velcade: U.S. FDA approval for the treatment of multiple myeloma progressing on prior therapy. *Oncologist* **8**, 508–513.
- [43] Orłowski RZ and Kuhn DJ (2008). Proteasome inhibitors in cancer therapy: lessons from the first decade. *Clin Cancer Res* **14**, 1649–1657.